

Probing Energy-Dependent Feshbach Resonances by Optical Control

N. Arunkumar¹, A. Jagannathan^{1,2}, and J. E. Thomas¹

¹*Department of Physics, North Carolina State University, Raleigh, NC 27695 and*

²*Department of Physics, Duke University, Durham, NC 27708*

(Dated: April 15, 2019)

Optical control enables new high resolution probes of narrow collisional (Feshbach) resonances, which are strongly dependent on the relative momentum of colliding atom pairs, and important for simulating neutron matter with ultracold atomic gases. We demonstrate a two-field optical vernier, which expands kHz (mG) magnetic field detunings near a narrow resonance into MHz optical field detunings, enabling precise control and characterization of the momentum-dependent scattering amplitude. Two-photon loss spectra are measured for the narrow resonance in ⁶Li, revealing rich structure in very good agreement with our theoretical model. However, anomalous frequency shifts between the measured and predicted two-photon spectra are not yet explained.

PACS numbers:

Magnetic Feshbach resonances [1] in ultracold gases have been extensively exploited to achieve important milestones in atomic physics, from the realization of strongly interacting Fermi systems [2–4] to the observation of Efimov trimers [5]. Typically, in a magnetic Feshbach resonance, an external magnetic field is used to tune the total energy of two colliding atoms in an energetically open channel into resonance with a bound dimer state in a closed channel. For a narrow Feshbach resonance, where the width is comparable to the relative energy of the incoming atom pair, the interactions are strongly momentum-dependent [6, 7]. This offers important possibilities for realizing novel quantum phases in ultracold gases, such as breached-pair superfluids [8].

Further, the large effective range r_e of narrow Feshbach resonances, coupled with resonant interactions, can be exploited to simulate neutron matter at sub-nuclear densities in the regime $k_F r_e \gtrsim 1$ (k_F is the Fermi momentum), which is an important regime for understanding the physics of neutron stars and supernova [9]. For the narrow Feshbach resonance in ⁶Li near 543.27 G (width $\Delta B \simeq 0.1$ G) r_e is anomalously large, $r_e \approx -7 \times 10^4 a_0$, with a_0 the Bohr radius [7, 10].

Previous experimental studies of narrow Feshbach resonances with momentum-dependent interactions have employed scans of external magnetic fields to create narrow Feshbach molecules [11], to measure two-body interactions [7], and to study three-body recombination loss [12]. Manipulation of Feshbach resonances also has been accomplished by using optical fields to tune the closed channel molecular bound state across the open channel continuum [13–21]. However, optical methods have had limited applicability due to atom loss arising from spontaneous scattering, which limits the tuning range.

Recently, we demonstrated optical control of interactions near the narrow Feshbach resonance in ⁶Li using closed-channel electromagnetically induced transparency [22]. In this scheme, two optical fields are used

to tune the closed channel molecular bound state near a magnetic Feshbach resonance with suppressed atom loss through destructive quantum interference [23, 24]. By tuning the frequency of one of the optical fields in our closed-channel EIT method, we vary the scattering length over the same range as achieved by magnetic tuning, and also control spatially varying interaction patterns in an ultracold atomic gas [25]. Our closed-channel EIT method also offers the possibility of creating synthetic FFLO states using momentum-selective control of interactions [26]. This requires a thorough understanding of optically controlled momentum dependent two-body interactions.

In this Letter, we report experiments on the narrow Feshbach resonance in ⁶Li, using the closed-channel EIT technique as a sensitive high-resolution probe of momentum dependent two-body interactions. Atom loss spectra are measured as a function of two photon-detuning for several magnetic fields, both on the atomic (BCS) side below the resonance and the molecular (BEC) side above the resonance. The spectra reveal a rich structure, which is strongly dependent on the magnetic field detuning. The spectra predicted by our momentum-dependent continuum-dressed state model are in excellent agreement with the data, both in shape and in absolute magnitude. However, we observe unexplained frequency shifts between the measured and predicted two-photon spectra, which are nearly constant at magnetic fields below resonance and strongly dependent on magnetic field above resonance.

The basic level scheme for our closed-channel EIT method is shown in Fig. 1. Optical fields ν_1 and ν_2 , with detunings Δ_1 and Δ_2 and Rabi frequencies Ω_1 and Ω_2 , couple the ground molecular states of the singlet potential, $|g_1\rangle$ and $|g_2\rangle$, to the excited state $|e\rangle$. A narrow Feshbach resonance arises from the second order hyperfine coupling V_{HF} between the bound state $|g_1\rangle$ and the triplet continuum $|T, k\rangle$, which tunes downward with increasing magnetic field B . We initially

choose a magnetic field such that the triplet continuum is tuned near $|g_1\rangle$, i.e., close to the resonance magnetic field $B_{res} = 543.27$ G [7, 25]. Near resonance, the optical detunings Δ_1 and Δ_2 are large compared to the magnetic detunings $\frac{2\mu_B}{\hbar}(B - B_{res})$, so that the two-photon detuning $\delta \simeq \Delta_2 - \Delta_1$. For $\delta = 0$, the light shift of $|g_1\rangle$ vanishes. As δ is varied from negative to positive, $|g_1\rangle$ tunes upward, from below to above its unshifted position. From Eq. 1 below, we find that this is equivalent to magnetically tuning $|T, k\rangle$ downward with a magnetic field of $\simeq -\frac{|\Omega_1|^2}{|\Omega_2|^2} \frac{\hbar \delta}{2\mu_B} \simeq -18 \text{ mG} \times \delta(\text{MHz})$ for our optical parameters. Hence, δ acts as an optical vernier to investigate the fine momentum-dependent features of the narrow Feshbach resonance. We note that the required magnetic field stability is the same as for magnetic tuning.

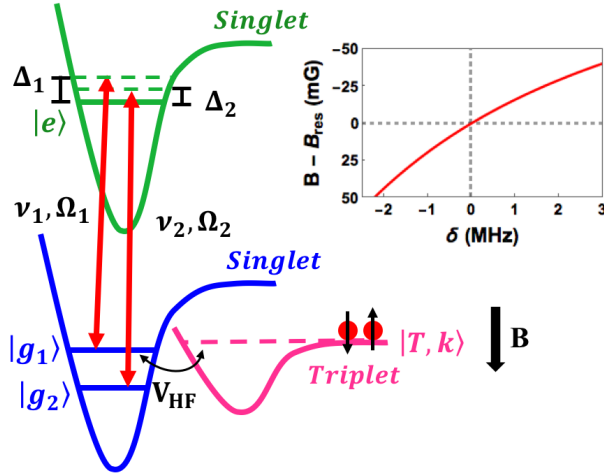


FIG. 1: Level scheme for closed-channel electromagnetically induced transparency (EIT). Optical fields ν_1 and ν_2 couple the ground molecular singlet states $|g_1\rangle$ and $|g_2\rangle$ with the excited singlet state $|e\rangle$ of the closed channel, resulting in a light shift of state $|g_1\rangle$. Atoms reside in the open channel triplet continuum $|T, k\rangle$, which is hyperfine coupled to $|g_1\rangle$, producing the narrow Feshbach resonance. Inset: The red line shows the effective magnetic tuning $B - B_{res}$, where $B_{res} = 543.27$ G, as a function of two-photon detuning δ (for $k = 0$). The horizontal dashed line, $B - B_{res} = 0$, corresponds to the unshifted position of $|g_1\rangle$ for $\delta = 0$. The energy of $|g_1\rangle$ tunes almost linearly with δ near the unshifted position, corresponding to a magnetic field tuning of $\simeq -18 \text{ mG} \times \delta(\text{MHz})$.

We begin with a cloud of ^6Li atoms, confined in a CO_2 laser trap, and prepared in a 50-50 mixture of the two lowest hyperfine states, $|1\rangle$ and $|2\rangle$. We evaporatively cool the atoms at 300 G to a temperature $T \simeq 2.0 \mu\text{K}$ in the nondegenerate regime and ramp the magnetic field to 528 G. An RF sweep (30 ms) then transfers the atoms from state $|2\rangle$ to state $|3\rangle$. The magnetic field is then ramped to the field of interest, where we wait 3 s for the magnetic field to stabilize. We then apply the ν_2 beam

with Rabi frequency $\Omega_2 = 2\pi \times 26$ MHz. We wait 30 ms for the atoms to reach equilibrium in the combined potential of the CO_2 laser and ν_2 beams. An RF π pulse (1.2 ms) then transfers the atoms from state $|3\rangle$ to state $|2\rangle$. The ν_1 beam with Rabi frequency $\Omega_1 = 2\pi \times 5.9$ MHz and detuning $\Delta_1 = +2\pi \times 19$ MHz is then applied for 5 ms. The atoms are imaged after a time of flight of $250 \mu\text{s}$, to determine the total atom number.

Fig. 2 and Fig. 3 show widely different atom loss spectra for magnetic fields above resonance $B > B_{res}$ (BCS side) and below resonance $B < B_{res}$ (BEC side). Atom loss is measured versus two-photon detuning δ , by varying ν_2 holding ν_1 constant. Atom loss arises from photoassociation of atoms in the triplet state $|T, k\rangle$, Fig. 1, where hyperfine coupling V_{HF} to $|g_1\rangle$ allows an optical transition to the excited singlet electronic state $|e\rangle$ and subsequent spontaneous emission. With increasing δ , the optical tuning of $|g_1\rangle$ is from below to above the triplet continuum, for each chosen B field. Comparing Fig. 2a, 30 mG above resonance, and Fig. 3a, 25 mG below resonance, we observe strikingly different spectral profiles, arising from the strongly momentum dependent scattering amplitude.

To understand the effects of momentum-dependent interactions on the spectra in Fig. 2 and Fig. 3, we compare the predictions of the continuum-dressed state model [27] for the k -averaged case (red solid line) to the zero momentum $k = 0$ case (green solid line). The momentum-averaged model captures the fine features of the measured spectral profiles. When the two-photon resonance condition is satisfied, i.e., $\delta \equiv 0$, atom loss is suppressed and the atom fraction $\simeq 1$. As noted above, for $\delta = 0$, the state $|g_1\rangle$ is also tuned to its original unshifted position. For both $B > B_{res}$ (Fig. 2) and $B < B_{res}$ (Fig. 3), maximum loss in the spectra occurs for δ values greater than the prediction of the zero momentum $k = 0$ model (green curves). This illustrates that maximum loss occurs when state $|g_1\rangle$ is optically tuned to be degenerate with the maximally occupied state $|T, k_0\rangle$ and not with $|T, 0\rangle$. When atoms with $k > k_0$ and with $k < k_0$ are near the molecular bound state $|g_1\rangle$, Fig. 4, the thermal momentum distribution averages positive and negative scattering amplitudes, resulting in a nearly zero mean field shift near resonance, as observed in the measurement of two-body interactions near a narrow Feshbach resonance [7].

Fig. 2a and Fig. 2b for $B > B_{res}$ show that the momentum-dependence of the scattering amplitude results in a second loss peak (red arrow) to the right of the minimum loss region (two-photon resonance $\delta = 0$), in agreement with the k -averaged theoretical model.

The spectral shapes are understood by considering the condition for maximum loss. From the momentum-dependent continuum dressed state model [27], Eq. S8,

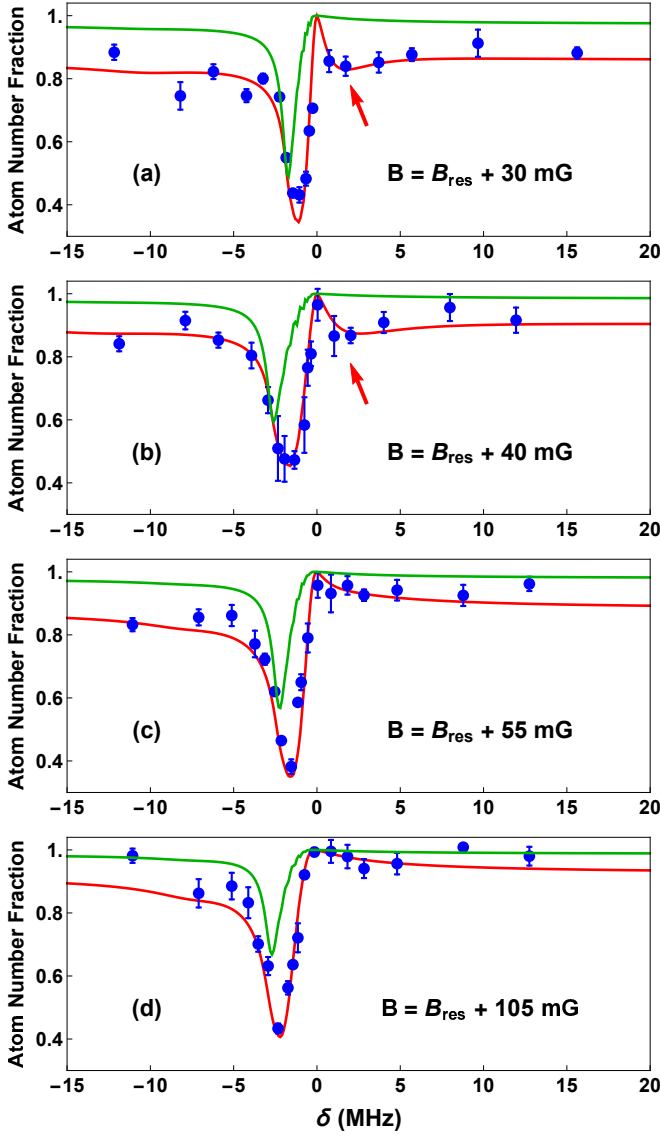


FIG. 2: Two-photon atom loss spectra for $B > B_{\text{res}}$. Atom number fraction (blue dots) as a function of two-photon detuning $\delta = \Delta_2 - \Delta_1$. $\delta \equiv 0$ denotes the two-photon resonance. Solid curves: Predictions from k -averaged (red) and $k = 0$ (green) theoretical model [27]. Note that the data is shifted horizontally (see Fig. 5) to align the measured minimum loss point with theoretical minimum loss point at $\delta \equiv 0$.

maximum loss occurs when

$$\Delta_1 + \frac{|\Omega_1|^2}{4 \left[\frac{2\mu_B}{\hbar} (B - B_{\text{res}}) - \frac{\hbar k^2}{m} \right]} + \frac{|\Omega_2|^2}{4\delta} = 0. \quad (1)$$

Here, we assume for brevity that the frequencies corresponding to the magnetic detuning $\frac{2\mu_B}{\hbar} (B - B_{\text{res}})$ and kinetic energy $\hbar k^2/m$, are small compared to the optical detunings Δ_1 and Δ_2 . For our experiments $\Delta_1 \approx +2\pi \times 19$ MHz. The second term is a one-photon optical shift arising from the k continuum [27]. In our experiments, where $\Omega_1 \approx 2\pi \times 5.9$ MHz, and $|B - B_{\text{res}}| < 0.1$ G,

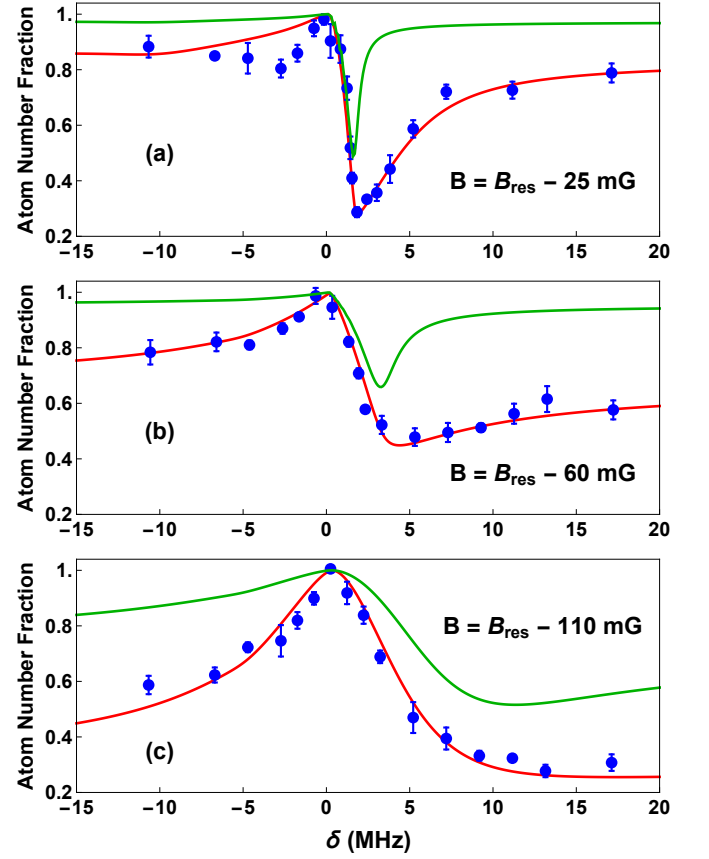


FIG. 3: Two-photon atom loss spectra for $B < B_{\text{res}}$. Atom number fraction (blue dots) as a function of two-photon detuning $\delta = \Delta_2 - \Delta_1$, by varying ν_2 and holding ν_1 constant. $\delta \equiv 0$ denotes the two-photon resonance. Solid curves: Predictions from k -averaged (red) and $k = 0$ (green) theoretical model [27]. Note that the data is shifted horizontally (see Fig. 5) to align the measured minimum loss point with theoretical minimum loss point at $\delta \equiv 0$.

this optical shift term is large compared to the Δ_1 term. Maximum loss therefore occurs when the one-photon optical shift is canceled by the two photon light shift given by the third term, where $\Omega_2 \simeq 2\pi \times 26$ MHz in our experiments. When $B < B_{\text{res}}$, the $|\Omega_1|^2$ term in Eq. 1 is negative for all k . Hence, the condition for maximum loss given by Eq. 1 is satisfied *only* when δ is positive, as we see in Fig. 3.

However, when $B > B_{\text{res}}$, the $|\Omega_1|^2$ term in Eq. 1 is positive for $k < k_r$ and negative for $k > k_r$, where k_r is the momentum of the triplet continuum state $|T, k_r\rangle$ that is degenerate with $|g_1\rangle$, which satisfies

$$\frac{2\mu_B}{\hbar} (B - B_{\text{res}}) - \frac{\hbar k_r^2}{m} = 0. \quad (2)$$

This leads to two loss peaks, a primary loss peak for $\delta < 0$ ($k < k_r$), due to the large atom population at lower k (Maxwell-Boltzmann distribution) and an additional loss peak (red arrow) for $\delta > 0$ ($k > k_r$), which is

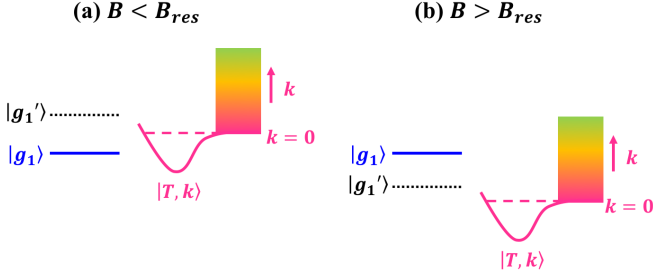


FIG. 4: (a) For $B < B_{res}$, the threshold of the triplet continuum $|T, k\rangle$ is above the unshifted position of $|g_1\rangle$. Hence, no occupied momentum states are resonant with the unshifted state $|g_1\rangle$. However, the light-shifted state $|g'_1\rangle$ can be tuned into resonance with thermally occupied $k > 0$ states. (b) For $B > B_{res}$, thermally occupied $k > 0$ states of the continuum are resonant with the unshifted state $|g_1\rangle$, provided that the magnetic detuning $\frac{2\mu_B}{\hbar}(B - B_{res})$ is comparable to the thermal energy $\frac{\hbar^2 k^2}{m}$. For $B < B_{res}$ ($B > B_{res}$), maximum loss occurs for $\delta > 0$ ($\delta < 0$), where $|g'_1\rangle$ is tuned above (below) the unshifted state $|g_1\rangle$ to be resonant with the maximally occupied triplet continuum state $|T, k\rangle$.

less populated, as we see in Fig. 2a and Fig. 2b. Note the momentum-dependent model captures the observed loss peak for $\delta > 0$, while the $k = 0$ model (green curve) is completely flat. As the magnetic detuning $B - B_{res}$ is increased, Eq. 2 can no longer be satisfied, since the momentum k_r is limited by the Maxwell-Boltzmann distribution for finite temperature T , i.e., $k < k_r$ for all k . Therefore, the additional loss peak for $\delta > 0$ disappears with increasing magnetic field detuning, as shown in Fig. 2c and Fig. 2d.

For $B < B_{res}$, Fig. 3, the unshifted bound state $|g_1\rangle$ lies below the triplet continuum and cannot resonantly couple with any k states. Then Eq. 2 is never satisfied, since the magnetic detuning term $B - B_{res}$ is negative and k is always positive. In this case, there is no additional loss peak near the two-photon resonance, since $|g_1\rangle$ is in its unshifted position for $\delta = 0$. However, the molecular bound state can be optically tuned to be resonant with non-zero k states by increasing δ . This appears as a long tail on the right side of the maximum loss peak in the spectra, where increasing δ scans $|g'_1\rangle$ through the thermal distribution of k states.

Although the shapes and magnitudes of the complex spectra are very well fit by our continuum dressed state model, we observe overall frequency shifts between the measured and predicted two-photon spectra shown in Fig. 2 and Fig. 3, which are unexplained. In the figures, the data has been frequency shifted, see Fig. 5, to align the measured minimum loss point with the theoretical minimum loss point at $\delta = 0$. For $B < B_{res}$, we observe that the required shift of the data, $\simeq -1.3$ MHz, is nearly independent of magnetic field, while for $B > B_{res}$, we observe a strong magnetic field dependence. The magnetic

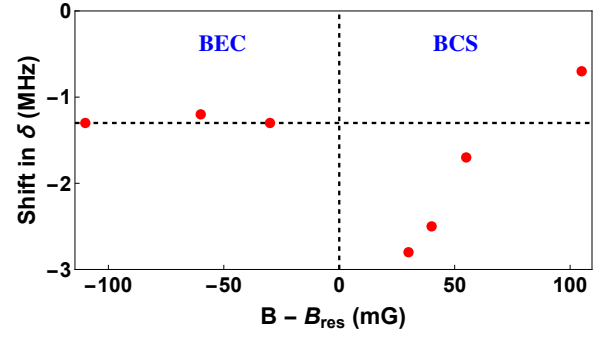


FIG. 5: Spectral shift of two-photon loss spectra (shown in Fig. 2 and Fig. 3) as a function of magnetic field B near the narrow Feshbach resonance at $B_{res} = 543.27$ G in ^6Li . The horizontal dashed line shows a background shift of $\simeq -1.3$ MHz. Vertical dashed line; $B = B_{res}$.

field independent shift may arise in part from a systematic error or from an anomalous background redshift of the excited state [13, 28], which would affect our Δ_1 frequency calibration and hence the absolute value of the two photon detuning δ . Such an anomalous shift was observed in the photoassociation experiments in ^7Li [29, 30], resulting in an overall spectral shift of the single-field atom loss spectra. An additional intensity-dependent asymmetric shift also was observed near a Feshbach resonance in ^7Li [31, 32]. As noted above, the one-photon optical shift term $\propto |\Omega_1|^2$ in Eq. 1 arises from the Feshbach resonance induced optical coupling of the triplet continuum to the excited state, and appears to explain the asymmetric shift observed in Ref. [31]. However, the frequency shifts observed in our experiments for the two-photon detuning are not explained and require further study.

In summary, we have studied momentum-dependent interactions for a narrow Feshbach resonance, by optically tuning the closed channel molecular bound state near the open channel continuum threshold. Using a closed-channel EIT method as an optical vernier, we observe that the momentum dependence of the two-body scattering amplitude strongly modifies the two-photon atom-loss spectra, providing new insights into energy-dependent Feshbach resonances.

-
- [1] C. Chin, R. Grimm, P. Julienne, and E. Tiesinga, Rev. Mod. Phys. **82**, 1225 (2010).
 - [2] K. M. O'Hara, S. L. Hemmer, M. E. Gehm, S. R. Granade, and J. E. Thomas, Science **298**, 2179 (2002).
 - [3] W. Ketterle and M. W. Zwierlein, *Making, probing and understanding ultracold Fermi gases* (IOS Press, Amsterdam, 2008), in Ultracold Fermi Gases, Proceedings of the International School of Physics Enrico Fermi, Course CLXIV, Varenna, 20 - 30 June 2006.
 - [4] I. Bloch, J. Dalibard, and W. Zwerger, Rev. Mod. Phys.

- 80**, 885 (2008).
- [5] T. Kraemer, M. Mark, P. Waldburger, J. G. Danzl, C. Chin, B. Engeser, A. D. Lange, K. Pilch, A. Jaakkola, H. C. Ngerl, et al., *Nature* **440**, 315 EP (2006).
 - [6] T.-L. Ho, X. Cui, and W. Li, *Phys. Rev. Lett.* **108**, 250401 (2012).
 - [7] E. L. Hazlett, Y. Zhang, R. W. Stites, and K. M. O'Hara, *Phys. Rev. Lett.* **108**, 045304 (2012).
 - [8] M. M. Forbes, E. Gubankova, W. V. Liu, and F. Wilczek, *Phys. Rev. Lett.* **94**, 017001 (2005).
 - [9] A. Schwenk and C. J. Pethick, *Phys. Rev. Lett.* **95**, 160401 (2005).
 - [10] H. Wu and J. E. Thomas, *Phys. Rev. A* **86**, 063625 (2012).
 - [11] K. E. Strecker, G. B. Partridge, and R. G. Hulet, *Phys. Rev. Lett.* **91**, 080406 (2003).
 - [12] J. Li, J. Liu, L. Luo, and B. Gao, *Phys. Rev. Lett.* **120**, 193402 (2018).
 - [13] P. O. Fedichev, Y. Kagan, G. V. Shlyapnikov, and T. M. Walraven, *Phys. Rev. Lett.* **77**, 2913 (1996).
 - [14] J. Bohn and P. Julienne, *Phys. Rev. A* **56**, 1486 (1997).
 - [15] F. Fatemi, K. Jones, and P. Lett, *Phys. Rev. Lett.* **85**, 4462 (2000).
 - [16] K. Enomoto, K. Kasa, M. Kitagawa, and Y. Takahashi, *Phys. Rev. Lett.* **101**, 203201 (2008).
 - [17] M. Theis, G. Thalhammer, K. Winkler, M. Hellwig, R. Grimm, and J. H. Denschlag, *Phys. Rev. Lett.* **93**, 123001 (2004).
 - [18] R. Yamazaki, S. Taie, S. Sugawa, and Y. Takahashi, *Phys. Rev. Lett.* **105**, 050405 (2010).
 - [19] D. M. Bauer, M. Lettner, C. Vo, G. Rempe, and S. Dürr, *Nat. Phys.* **5**, 339 (2009).
 - [20] M. Jag, M. Zaccanti, M. Cetina, R. S. Lous, F. Schreck, R. Grimm, D. S. Petrov, and J. Levinsen, *Phys. Rev. Lett.* **112**, 075302 (2014).
 - [21] L. W. Clark, L.-C. Ha, C.-Y. Xu, and C. Chin, *Phys. Rev. Lett.* **115**, 155301 (2015).
 - [22] A. Jagannathan, N. Arunkumar, J. A. Joseph, and J. E. Thomas, *Phys. Rev. Lett.* **116**, 075301 (2016).
 - [23] H. Wu and J. E. Thomas, *Phys. Rev. Lett.* **108**, 010401 (2012).
 - [24] H. Wu and J. E. Thomas, *Phys. Rev. A* **86**, 063625 (2012).
 - [25] N. Arunkumar, A. Jagannathan, and J. E. Thomas, *arXiv:1803.01920* (2018).
 - [26] L. He, H. Hu, and X.-J. Liu, *Phys. Rev. Lett.* **120**, 045302 (2018).
 - [27] See the Supplemental Material in [22] for a more detailed description of the experimental methods and of our continuum dressed state model.
 - [28] J. L. Bohn and P. S. Julienne, *Phys. Rev. A* **60**, 414 (1999).
 - [29] I. D. Prodan, M. Pichler, M. Junker, R. G. Hulet, and J. L. Bohn, *Phys. Rev. Lett.* **91**, 080402 (2003).
 - [30] J. M. Gerton, B. J. Frew, and R. G. Hulet, *Phys. Rev. A* **64**, 053410 (2001).
 - [31] M. Junker, D. Dries, C. Welford, J. Hitchcock, Y. P. Chen, and R. G. Hulet, *Phys. Rev. Lett.* **101**, 060406 (2008).
 - [32] M. Mackie, M. Fenty, D. Savage, and J. Kesselman, *Phys. Rev. Lett.* **101**, 040401 (2008).